doi:10.1006/mthe.2001.0457, available online at http://www.idealibrary.com on IDEAL

ARTICLE

Infection of Purified Nuclei by Adeno-associated Virus 2

Jonathan Hansen,[1,2,4] Keyun Qing,[1,2,4] and Arun Srivastava[1–4,*]

[1]Department of Microbiology & Immunology, [2]Walther Oncology Center, [3]Division of Hematology/Oncology, Department of Medicine, Indiana University School of Medicine, and [4]Walther Cancer Institute, Indianapolis, Indiana 46202, USA

*To whom correspondence and reprint requests should be addressed. Fax: (317) 274-4090. E-mail address: asrivast@iupui.edu.

Adeno-associated virus 2 (AAV), a nonpathogenic human parvovirus, requires co-infection with a helper virus for its optimal replication. Although AAV possesses a broad host range, certain cell types lack the machinery necessary for efficient entry into the cell and intracellular trafficking of AAV into the nucleus, where the viral second-strand DNA synthesis must occur before gene expression. We have demonstrated that in less-permissive mouse fibroblasts, the virus fails to transport to the nucleus due to altered endocytic processing. However, relatively little is known about the intracellular site of viral uncoating and transport of the virion across the nuclear envelope. Here, we provide evidence that AAV can efficiently enter intact nuclei purified from both permissive and less-permissive cell types. Furthermore, entry into the nucleus is time- and temperature-dependent, but is not saturable and seems to occur independently of the nuclear pore complex. We also demonstrate that purified nuclei contain all of the machinery necessary for uncoating and viral second-strand DNA synthesis even in the absence of a helper virus. These studies provide new insights into the basic biology of AAV and may also have implications for the optimal use of AAV vectors in human gene therapy.

Key Words: AAV, trafficking, uncoating, nucleus, nuclear pore complex, DNA synthesis

INTRODUCTION

Adeno-associated virus 2 (AAV) is a small (~ 26 nm), nonenveloped, nonpathogenic human parvovirus containing single-stranded DNA that requires co-infection with a helper virus such as adenovirus for its optimal replication [1,2]. In the absence of a helper virus, the wild-type AAV binds to and enters the target cell and then transports into the nucleus to use the host DNA replication machinery to synthesize the viral second-strand DNA, and the viral genome integrates relatively site-specifically into human chromosome 19 [3]. Although recombinant AAV vectors seem to lack the site-specificity of integration, their nonpathogenic nature and their ability to infect both quiescent and dividing cell types from multiple species have been instrumental in their use as vectors in gene therapy. Indeed, AAV vectors are currently in use in phase II clinical trials to correct the genetic defects in cystic fibrosis and hemophilia B [4,5].

Despite a wide host range, AAV vectors do not transduce all cell types equally. For instance, whereas muscle, brain, and liver cells are transduced very efficiently, human megakaryocytic and lymphoblastic cell lines have been shown to be nonpermissive for infection by AAV because they lack the necessary viral receptor and/or coreceptors [6–9]. Other cell types, such as human airway epithelia, have been identified that are minimally permissive for AAV infection because they degrade incoming virions by means of the ubiquitin-proteasome pathway [10]. The efficiency of transduction in permissive cells has also been shown to be modulated by a cellular protein, designated FKBP52, phosphorylated forms of which bind near the 3′ end of the AAV genome and prevent the viral second-strand DNA synthesis and therefore transgene expression [11–13].

More recently, we have identified an additional obstacle to efficient AAV-mediated transduction of mouse fibroblasts [14,15]. Although AAV efficiently binds and enters these cells, it fails to transport into the nucleus due to altered endocytic processing. Treatment of these cells with hydroxyurea (HU), an inhibitor of ribonucleotide reductase, has been shown to restore endocytic processing through the late endosomes and therefore increase trafficking of the virus into the nucleus [15].

Whereas some of the steps involved in the intracellular trafficking of AAV through the endocytic compartment have become clearer in various cell types, relatively little is known about how the virus enters the nucleus. It is also not known precisely where the viral uncoating occurs. We and others have previously shown that AAV DNA can be detected in the nucleus as early as 2 hours postinfection [14,16]. Furthermore, AAV capsid proteins have also been shown to enter the nucleus [16,17], but direct evidence

1525-0016/01 $35.00

doi:10.1006/mthe.2001.0457, available online at http://www.idealibrary.com on IDEAL

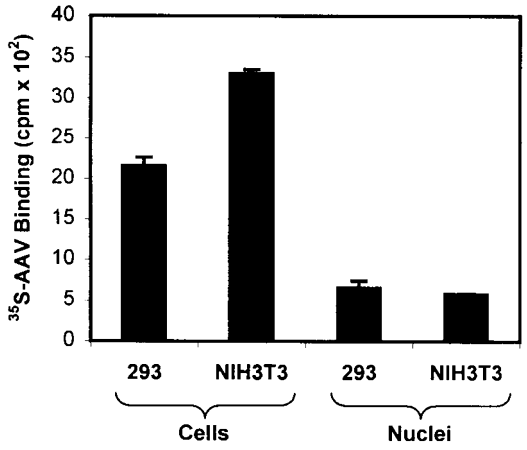

FIG. 1. Binding of ^{35}S-AAV to cells and isolated nuclei. Cells or nuclei were incubated with ^{35}S-labeled AAV and cell- and nucleus-associated radioactivity was measured. Values expressed are the average of three experiments and error bars represent one standard deviation.

that uncoating of the virion actually occurs within the nucleus is lacking. Moreover, the pathways involved in transport across the nuclear membrane remain to be determined.

Here, we present evidence that AAV enters nuclei purified from both permissive and less-permissive cell types to a similar degree in a time- and temperature-dependent manner. The viral entry is not inhibited by excess unlabeled AAV, nor by basic fibroblast growth factor (bFGF), both of which inhibit binding of AAV to the cell surface receptor and co-receptor [7,9]. The viral entry also does not seem to be mediated by the nuclear pore complex (NPC), but all of the machinery necessary for viral entry into the nucleus—uncoating and second-strand DNA synthesis—are contained within the nucleus. These studies establish that AAV enters the cell nucleus intact.

RESULTS

AAV Binds to and Enters Purified Nuclei

We carried out a systematic analysis of the binding and entry of AAV in nuclei purified from 293 and NIH3T3 cells, permissive and less-permissive cell types, respectively. We incubated ^{35}S-labeled AAV with equivalent numbers of intact cells and purified nuclei at 4°C, after which we determined the cell- and nucleus-associated radioactivity. Consistent with our previous results, AAV bound to NIH3T3 cells slightly better than to 293 cells [7] (Fig. 1). However, AAV associated approximately 75% less efficiently with the nuclei from both cell types than with intact cells.

We also examined the time- and temperature-dependence of AAV entry into nuclei. It has previously been established that binding of AAV to the cell surface receptor on intact cells, but not internalization, occurs at 4°C [16]. To determine if the same was true for nuclei, we incubated Cy3-fluorochrome-labeled AAV, generated by a described method [18], with nuclei purified from 293 or NIH3T3 cells at 4°C or 37°C for 15 or 90 minutes. We then visualized the nuclear-associated AAV by confocal microscopy. Unlike in intact cells, Cy3–AAV (red signal) was able to enter the nuclei at 4°C after 15 minutes (Figs. 2A and 2E); and by 90 minutes, the amount of internalized virus had increased (Figs. 2B and 2F). Similarly, at 37°C, Cy3–AAV was visualized within the nuclei after 15 minutes (Figs. 2C and 2G) albeit at higher levels, and there was no significant change in internalized virus after 90 minutes (Figs. 2D and 2H). Because AAV entered nuclei but not cells at 4°C, these data indicate that AAV enters cells and nuclei by distinct mechanisms. Moreover, these results demonstrate that AAV entry into nuclei is time- and temperature-dependent and that there is no detectable difference in entry between nuclei isolated from permissive versus less-permissive cell types.

We confirmed the integrity of the nuclear envelope in the nuclei used in these experiments as follows. We incubated the nuclei purified from 293 cells under identical conditions to those described for data shown in Fig. 2, and then mounted them in medium containing FITC-conjugated dextrans with an average molecular mass of either 4 or 150 kDa, after which we visualized the nuclei by confocal microscopy. The 4-kDa dextrans freely permeated the nuclei (Fig. 3A), whereas the 150-kDa dextrans were excluded (Figs. 3B–3E) under each of the conditions tested. These results confirm that the nuclear envelopes were intact and that the results shown in Fig. 2 were not due to passage of the virions through lesions in the nuclear envelope. We obtained similar results with nuclei purified from NIH3T3 cells (data not shown).

Entry of AAV into Nuclei Is Not Saturable and Is Not Mediated by the NPC

Because AAV enters purified nuclei, we hypothesized that some type of nuclear receptor distinct from the cellular receptors might mediate viral entry. To this end, we performed a series of experiments in which nuclei from both 293 and NIH3T3 cells were incubated with ^{35}S-AAV in the presence or absence of various competitors. Competition with 50-fold excess unlabeled AAV did not substantially decrease entry of AAV into the nuclei (Fig. 4A), indicating that the import mechanism was not saturable. We also confirmed these results in confocal microscopy experiments with 100-fold excess unlabeled AAV (data not shown). Furthermore, although bFGF has been shown to inhibit binding of AAV to the cell surface receptors [7], it was unable to effectively reduce entry into the nuclei. Competition studies using heparin, which also inhibits binding of AAV to the cell surface [8], were unsuccessful due to the instability of the nuclei in the presence of

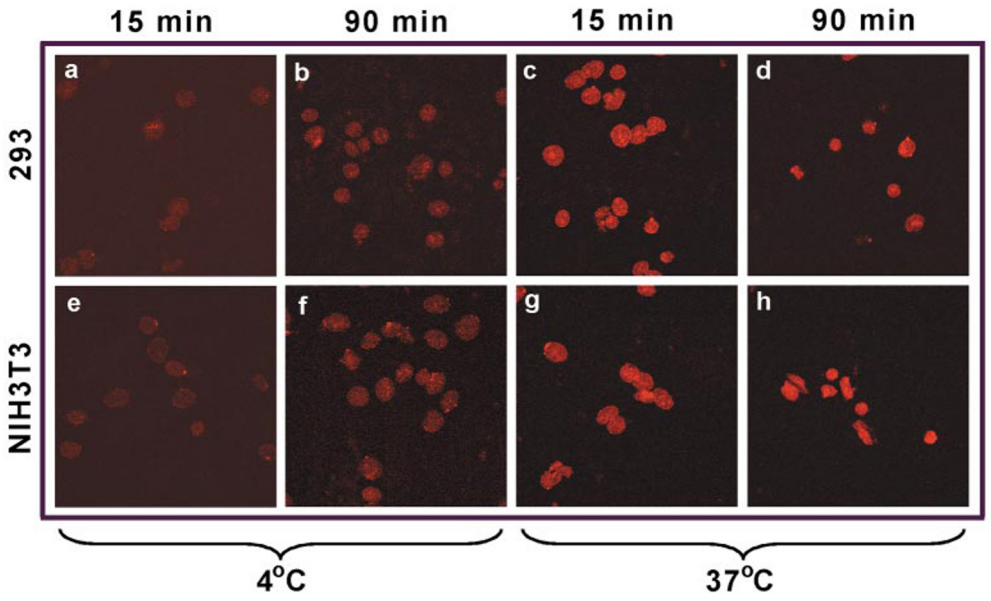

FIG. 2. Confocal microscopy for Cy3–AAV entry in isolated nuclei. Nuclei from 293 or NIH3T3 cells were incubated with Cy3–AAV for the indicated times at the indicated temperatures. Cy3–AAV (red) was visualized by confocal microscopy.

heparin. The best-characterized system of nuclear import in intact cells involves the NPC and an antibody specific for one of the proteins in the NPC, p62, has been shown to block NPC-mediated import [19]. However, entry of AAV into the nuclei was unaltered in the presence of this antibody (Fig. 4A). To further rule out the involvement of NPC, we pretreated the nuclei with wheat germ agglutinin (WGA), a compound known to block NPC-mediated import by binding to *O*-linked *N*-acetylglucosamine residues on proteins of the NPC [20], followed by incubation with Cy3–AAV. By confocal microscopy, it is evident that WGA did not reduce viral entry into nuclei from either cell type (Fig. 4B). We did confirm the binding of WGA to the NPC by confocal microscopy using FITC-labeled WGA (data not shown). These data were as expected, as cytoplasmic factors not present in our system are essential for "classical" NPC-mediated import. Furthermore, pretreatment of cells with compounds that deplete the endoplasmic reticulum of calcium, and which have been shown to cause closure of the NPC [21], had no effect on AAV-mediated transduction (data not shown). Based on these results, we conclude that AAV enters the nucleus in a non-saturable manner by a novel pathway that does not seem to use the NPC.

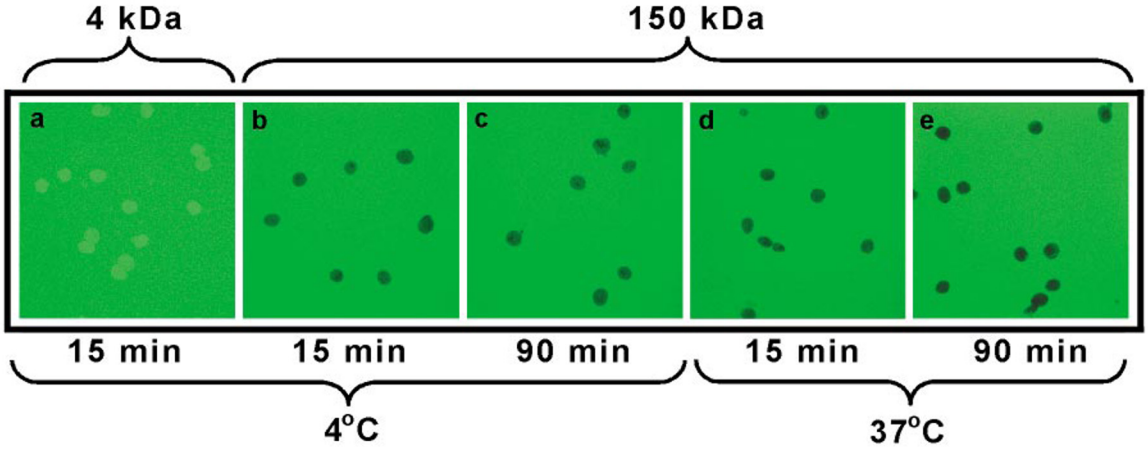

FIG. 3. Assessment of nuclear envelope integrity. Nuclei from 293 cells were incubated for the indicated times and temperatures and mounted in medium containing FITC-labeled dextrans with a mass of either 4 kDa or 150 kDa and were then visualized by confocal microscopy.

doi:10.1006/mthe.2001.0457, available online at http://www.idealibrary.com on IDEAL

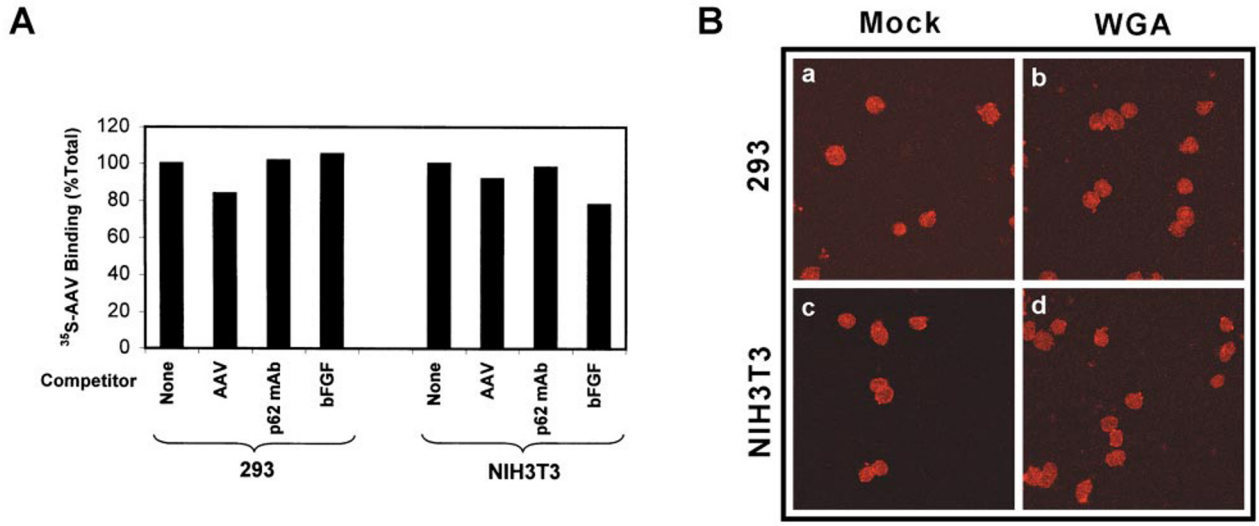

FIG. 4. Competition of binding and entry into isolated nuclei. (A) Nuclei were pre-incubated with medium alone (None), 50-fold excess of unlabeled AAV (AAV), 1 μg of anti-p62 (p62 mAb), or 5 μg of bFGF for 30 min on ice followed by the addition of ^{35}S-AAV. Nuclear-associated ^{35}S-AAV was then quantified. Values are presented as a percentage of the total binding when no competitor was present and represent the average of three experiments. (B) Nuclei from 293 or NIH3T3 cells were pre-incubated with or without wheat germ agglutinin (WGA) and then incubated with Cy3–AAV. Nuclear-associated Cy3–AAV was then visualized by confocal microscopy.

Purified Nuclei Contain All of the Factors Required for Viral Entry, Uncoating, and Second-Strand DNA Synthesis

Although we and others have established that AAV capsids labeled with either ^{35}S or a Cy3 fluorochrome localize to the nucleus [10,14,17], the integrity of the virions and their ability to uncoat and undergo viral second-strand DNA synthesis have not been directly demonstrated. To this end, we developed an assay to measure the viral second-strand DNA synthesis in nuclei purified from AAV infected cells. We either mock-infected or infected 293 cells with AAV or Ad2 (10 multiplicity of infection (MOI)) alone, or co-infected with AAV and Ad2, after which we isolated the nuclei from these cells and incubated in the presence of dNTPs and α^{32}P-dCTP. We isolated low M_r DNA from the nuclei, separated on agarose gels, and transferred to a nylon membrane followed by autoradiography. In all lanes, the radiolabel was incorporated into the high M_r genomic (g) DNA that copurified with the low M_r DNA (Fig. 5), indicating that the cellular DNA replication was functional under these conditions. The monomeric (m) replicative form of the viral genome was only detected 48 hours after co-infection with Ad2 and AAV (Fig. 5, lane 4). Upon overexposure, a signal representing the monomer was also detected 24 hours after co-infection (data not shown), but no signal was observed in cells infected with either AAV alone (Fig. 5, lane 2) or Ad2 alone (Fig. 5, lane 5). These data demonstrate that AAV second-strand DNA synthesis occurs in the nucleus, which can be readily detected under these *in vitro* conditions.

We next determined whether, following entry, AAV might also undergo uncoating and viral second-strand DNA synthesis within the purified nuclei. To test this, we isolated nuclei from 293 or NIH3T3 cells and either mock-infected or infected them with AAV, and measured the viral second-strand DNA synthesis as described above. No monomeric form was detected in mock-infected nuclei

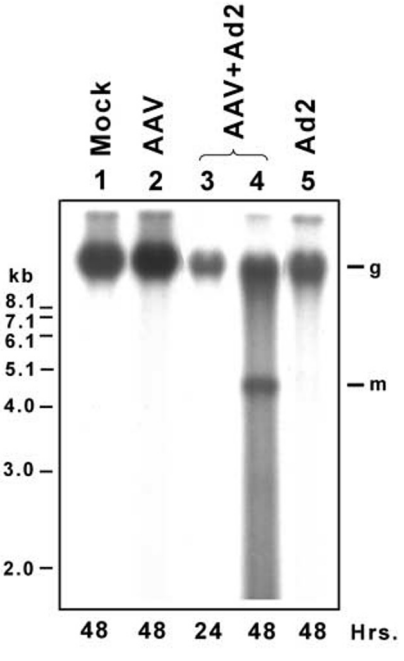

FIG. 5. AAV second-strand DNA synthesis in nuclei from infected 293 cells. Cells were either mock infected, infected with AAV, Ad2, or co-infected with AAV and Ad2. At the indicated time points, the incorporation of α^{32}P-dCTP into replicating DNA in nuclei isolated from these cells was measured. The positions of genomic (g) DNA and viral monomeric (m) DNA are indicated.

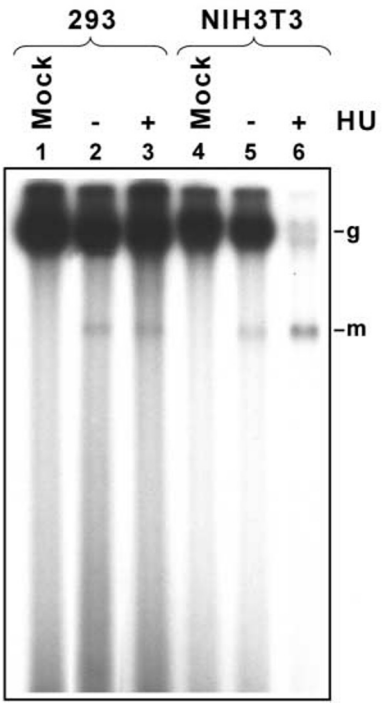

FIG. 6. Viral second-strand DNA synthesis in purified nuclei infected by AAV. The 293 or NIH3T3 cells were mock-treated or treated with 10 mM hydroxyurea (HU). After 24 h, nuclei purified from these cells were incubated with AAV, and viral second-strand DNA synthesis was detected.

from either cell type (Fig. 6, lanes 1 and 4), as expected. However, monomeric forms were detected in AAV-infected nuclei isolated from both cell types (Fig. 6, lanes 2 and 5). To rule out the possibility that the observed monomeric forms of AAV DNA did not result from repair synthesis, we electrophoresed the replication products from mock-infected and AAV-infected nuclei from both cell types on alkaline-agarose gels followed by autoradiography. Fragments larger than the unit-length AAV genomes were detected in infected nuclei from both cell types (Fig. 7), indicating that the monomeric forms detected represent true viral second-strand DNA synthesis rather than repair synthesis of two annealed complementary AAV genomes.

To further substantiate that the nuclear membrane integrity was maintained under the conditions used to detect the viral second-strand DNA synthesis, we incubated the nuclei purified from 293 cells under identical conditions (15 min at 37°C to mimic AAV infection followed by 5 h at 25°C to mimic viral DNA replication) and mounted them in medium containing FITC-labeled dextrans. We then visualized the nuclei by confocal microscopy. The 4-kDa dextrans freely permeated the nuclei (Fig. 8), but 150-kDa dextrans were excluded, confirming that, under the conditions used to detect the viral second-strand DNA synthesis, the nuclei maintained their structural integrity. We obtained similar results with nuclei isolated from NIH3T3 cells (data not shown). These data corroborate that AAV can indeed infect nuclei isolated from both permissive and less-permissive cells, uncoat, and undergo second-strand DNA synthesis to a similar extent. Furthermore, all factors necessary for these processes are contained within the nucleus because the nuclear preparations were free from cytoplasmic contaminants.

Factors in Addition to the Cellular FKBP52 Protein Mediate Viral Second-Strand DNA Synthesis

We have documented that treatment of cells with hydroxyurea (HU) increases AAV-mediated transduction, most likely by causing dephosphorylation of the cellular FKBP52 protein, resulting in increased viral second-strand DNA synthesis [11–13]. We postulated, therefore, that treatment of 293 or NIH3T3 cells with HU before isolation and infection of the nuclei might increase the amount of radiolabel incorporated into the monomeric form of viral DNA. To test this hypothesis, we purified nuclei from 293 or NIH3T3 cells that had been mock-treated or treated with 10 mM HU for 24 hours. After infecting the nuclei with AAV, we measured viral second-strand DNA synthesis as described above. The amount of viral second-strand DNA synthesis increased in AAV-infected nuclei that were isolated from HU-treated cells (Fig. 6, lanes 3 and 6) relative to untreated cells (Fig. 6, lanes 2 and 5). Densitometric scanning of autoradiographs from three separate experiments revealed an average increase in signal intensities in response to HU treatment of 1.3 and 2.0 for 293 and NIH3T3 cells, respectively. Therefore, we conclude that HU treatment increases viral second-strand DNA synthesis in purified nuclei.

As we have shown that dephosphorylation of FKBP52 at tyrosine residues enhances the rate of viral second-strand DNA synthesis [11–13], we reasoned that HU

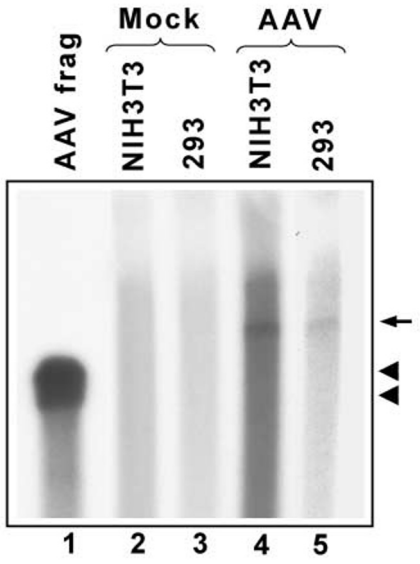

FIG. 7. Alkaline-agarose gel electrophoresis of AAV DNA replication products. Purified nuclei from NIH3T3 and 293 cells were either mock-infected (lanes 2 and 3) or infected with AAV (lanes 4 and 5) and the viral second-strand DNA synthesis was carried out as described in Fig. 5, except low M_r DNA samples were electrophoresed under denaturing conditions. The *Xba*I fragment, containing the 4.4-kb AAV genome without the viral inverted terminal repeats, was derived from plasmid pSub201, end-labeled with ^{32}P, and used as a size marker (lane 1). The arrowheads indicate the two strands of the AAV genome, and the arrow denotes the viral second-strand DNA synthesis product.

doi:10.1006/mthe.2001.0457, available online at http://www.idealibrary.com on IDEAL

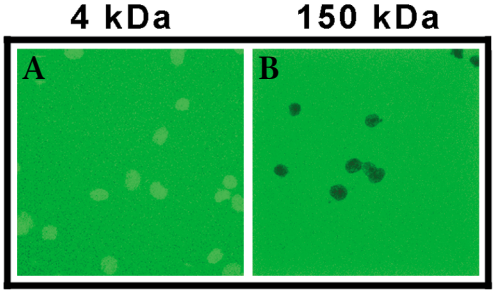

FIG. 8. Assessment of nuclear envelope integrity under the conditions of the viral second-strand DNA synthesis. Purified nuclei from 293 cells were incubated at 37°C for 30 min followed by incubation at 25°C for 5 h, mounted in medium containing FITC-labeled dextrans with a mass of either 4 kDa (A) or 150 kDa (B), and visualized by confocal microscopy.

treatment causes dephosphorylation of FKBP52 resulting in the increased rate of the viral second-strand DNA synthesis (Fig. 6). To test this, we carried out electrophoretic mobility shift assays with ^{32}P-labeled AAV D-sequence oligonucleotide probe and extracts prepared from purified nuclei as described [11,12]. Consistent with our previously published studies [11,12], FKBP52 in nuclei from untreated 293 cells (Fig. 9, lane 2) was present in predominantly the serine/threonine-phosphorylated form and did not undergo any change upon treatment of cells with HU (Fig. 9, lane 3). In contrast, FKBP52 in nuclei purified from untreated NIH3T3 cells (Fig. 9, lane 4) migrated slower (arrow), representing the tyrosine-phosphorylated form of the protein. Treatment of NIH3T3 cells with HU (lane 5) resulted in tyrosine dephosphorylation, which is consistent with the approximately twofold increase in viral second-strand DNA synthesis in nuclei from HU-treated NIH3T3 cells (Fig. 6, lane 6). However, because we detected similar amounts of monomeric viral DNA in nuclei from untreated 293 and NIH3T3 cells, it seems that, in addition to the phosphorylation status of FKBP52, other factors are also involved in catalyzing the synthesis of the second strand of the AAV genome.

DISCUSSION

More than two decades ago, it was suggested that intact AAV particles enter the cell nucleus, where they undergo uncoating [22]. However, direct experimental evidence to document transport of the virion from the cytoplasm through the nuclear envelope into the nucleus and the role of these steps in the viral life cycle has been lacking.

Here, we have systematically explored the events surrounding nuclear entry and viral second-strand DNA synthesis. First, we demonstrated that binding and entry of AAV into nuclei is time- and temperature-dependent, is not saturable, and cannot be abrogated by agents that block NPC function. Second, we directly showed that during a "natural" infection of intact cells by AAV, viral second-strand DNA synthesis occurs in the nucleus. Third, we provided evidence that AAV can infect purified nuclei, uncoat, and synthesize the viral second strand of DNA, indicating that cellular factors required for these functions are localized entirely within the nucleus.

Although most of the factors that dictate permissiveness for AAV infection are cell-type specific, we showed that entry into the nucleus and viral second-strand DNA synthesis do not seem to limit AAV-mediated transduction of the less-permissive NIH3T3 cells compared with the more permissive 293 cells. We have reported that AAV fails to be transported by means of acidified vesicles in NIH3T3 cells, a prerequisite for subsequent nuclear localization of the virions [15]. We have proposed that passage through the acidic compartment exposes the virion to conditions that modify the capsid, allowing for transport into the nucleus [15]. In the present studies, however, we were able to infect purified nuclei with unmodified AAV virions indicating that the putative capsid change that occurs in the acidic compartment affects trafficking steps before nuclear entry. Because it has been demonstrated that AAV-mediated transduction and nuclear localization require an intact microtubule network, perhaps the capsid modification enables virions to use the cytoskeleton for

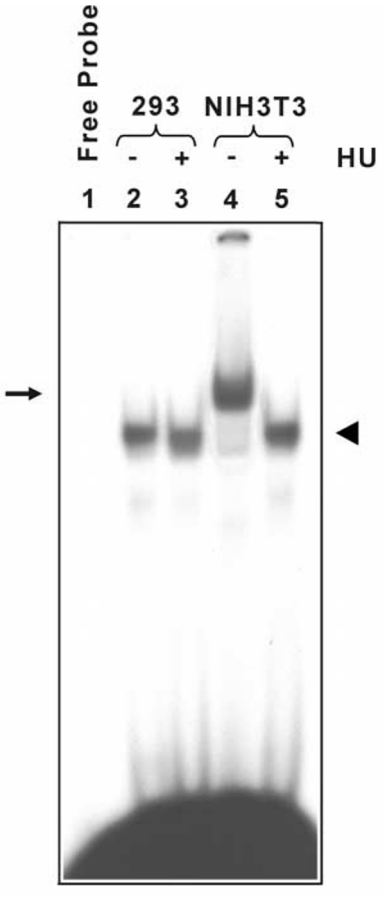

FIG. 9. Electrophoretic mobility shift assay for the phosphorylation status of FKBP52. The 293 or NIH3T3 cells were either mock-treated or treated with 10 mM HU. After 24 h, nuclear extracts from these cells were prepared and used in electrophoretic mobility shift assays. Phosphorylated and dephosphorylated forms of FKBP52 are indicated by the arrow and the arrowhead, respectively.

subsequent trafficking events to the nucleus [16]. Further studies are needed to gain a better understanding of cytoplasmic trafficking of AAV.

Transport across the nuclear envelope has been extensively studied for many cellular proteins and some viruses [23]. Most models include a role for the NPC, a multi-subunit complex that spans the bilaminar nuclear envelope and opens and closes to allow for transit into and out of the nucleus. The NPC allows macromolecules < 30–40 kDa to freely diffuse across the nuclear envelope and, in certain cases, it can open to accommodate particles as large as 28 nm [23]. Given that the diameter of AAV virions is 26 nm, it is feasible that they could pass into the nucleus through the NPC. However, agents known to block active NPC-mediated transport did not inhibit viral entry into the nucleus. Furthermore, NPC-mediated transport requires certain cytoplasmic factors and does not occur at 4°C [24]. Despite the lack of cytoplasmic factors in our experiments, we still observed nuclear entry, even at 4°C. Thus, we conclude that AAV enters the nucleus either through the NPC using an unknown mechanism or viral entry into the nucleus is independent of the NPC. We favor the latter hypothesis because the entry seems to be nonsaturable.

We have demonstrated the ability of AAV to infect nuclei isolated from permissive as well as less-permissive cells, uncoat, and synthesize the second-strand of its genome. These studies, although distinctly different from viral infection of intact cells, lay the groundwork for further investigations into novel mechanisms of nuclear transport of viruses in general and AAV in particular. Elucidation of these steps in viral infection at the molecular level will add to our current overall understanding of the basic biology of AAV, which in turn will improve its usefulness as a vector for human gene therapy.

MATERIALS AND METHODS

Cells and viruses. The adenovirus-transformed human embryonic kidney cell line 293 and the mouse fibroblast cell line NIH3T3 were obtained from the American Type Culture Collection (Rockville, MD). Recombinant AAV vectors were prepared and labeled with Cy3 Reactive Dye (Amersham, Pittsburgh, PA) as described [7,18]. ^{35}S-labeled wild-type AAV stocks were generated and purified as described [7]. Adenovirus 2 (Ad2) stocks were kindly supplied by Kenneth H. Fife (Indiana University School of Medicine, Indianapolis, IN).

Purification of nuclei. Nuclei from actively dividing 293 and NIH3T3 cells were purified according to a modified method [25]. All procedures were carried out at 4°C. The 293 cells were washed once in PBS and once in hypotonic buffer (10 mM HEPES, pH 7.6, 25 mM KCl, 2 mM magnesium acetate, 1 mM DTT, 0.1 mM PMSF), incubated on ice for 5 min, and homogenized in 1 ml hypotonic buffer in a tight-fitting Duall tissue grinder (Fisher Scientific, Pittsburgh, PA) until ~ 80% cell lysis was achieved (~ 20 strokes). The lysate was diluted to 9 ml with adjusting solution (1.22 M sucrose, 10 mM HEPES, pH 7.6, 5 mM magnesium acetate, 1 mM DTT, 0.1 mM EDTA, and 0.1 mM PMSF), layered onto 3 ml of a sucrose cushion (1.8 M sucrose, 10 mM HEPES, pH 7.6, 5 mM magnesium acetate, 1 mM DTT, 0.1 mM EDTA, and 0.1 mM PMSF), and centrifuged in an SW41Ti rotor (Beckman) at 14,000 rpm for 1 h at 4°C. The supernatant was aspirated and the nuclear pellet washed. Nuclei from NIH3T3 cells were isolated as above except the hypotonic buffer was substituted with homogenization buffer (0.25 M sucrose, 10 mM triethanolamine, pH 7.6, 1 mM EDTA, 0.1 mM PMSF) due to the resistance of NIH3T3 cells to hypotonic-mediated cell lysis. Purity of nuclei was determined as described by the absence of acid β-galactosidase activity, a lysosomal enzyme [14]. Nuclei were stored on ice and used within 2 h. Integrity of the nuclear envelope was confirmed by exclusion of 150-kDa dextran molecules but not 4-kDa dextrans as described [26]. Briefly, nuclei were incubated for various indicated times and temperatures, adhered to coverslips, fixed, mounted in medium containing 2 μM FITC-conjugated dextrans (Sigma, St. Louis, MO), incubated at 25°C for 18 h, and then visualized by confocal microscopy.

Confocal microscopy for Cy3-labeled AAV binding and entry. Approximately 1×10^5 nuclei were incubated with 20,000 particles per nucleus of Cy3–AAV for the indicated times and at the indicated temperatures in 25 μl IMDM containing 0.1% BSA. During the final 15 min of incubation, the sample was transferred to a 35-mm tissue culture dish containing a coverslip that had been coated with Cell-Tak Cell and Tissue Adhesive (Collaborative Biomedical Products, Bedford, MA) according to the manufacturer's instructions. After a brief (~ 5 s) spin at 500 rpm in a Beckman GPKR centrifuge, the coverslip was immediately washed three times with 2 ml PBS and fixed on ice for 30 min in PBS containing 2% formaldehyde and 0.2% glutaraldehyde. Coverslips were then mounted in a PBS:glycerol mixture (1:1) onto glass slides and fluorescence was visualized on a Zeiss LSM 510 confocal microscope. Images are representative of a 0.7–1.0 μm slice through the centers of the nuclei and were obtained using a ×63 objective with water correction. In some experiments, nuclei were preincubated with 200 μg/ml of WGA (Sigma, St. Louis, MO) for 10 min at 25°C before the addition of the Cy3–AAV.

^{35}S-AAV binding and entry assays. Approximately 1.5×10^6 nuclei were incubated with 17,000 cpm of ^{35}S-AAV in a final volume of 100 μl IMDM containing 0.1% BSA on ice for 90 min. In some experiments, before the addition of the ^{35}S-AAV, nuclei were preincubated for 30 min on ice with one of the following: a 50-fold excess of unlabeled AAV; 1 μg anti-p62 monoclonal antibody (Santa Cruz Biotechnology, Santa Cruz, CA); or 5 μg bFGF (Sigma, St. Louis, MO). Nuclei were then washed three times in IMDM containing 1.5% BSA, transferred to 10 ml scintillation fluid, and the activity counted in a scintillation counter. All experiments were carried out in triplicate. AAV binding to an equivalent number of intact cells was measured as described [7].

Electrophoretic mobility shift assays. Nuclei from NIH3T3 and 293 cells were purified as above and washed with PBS, after which nuclear extracts were prepared as described [11]. Protein concentrations were determined using the Bio-Rad Protein Assay (Bio-Rad, Hercules, CA) according to the manufacturer's instructions and 10 μg of total protein was used in electrophoretic mobility shift assays as described [11].

Viral second-strand DNA synthesis assays in purified nuclei. Nuclei purified from 293 or NIH3T3 cells were washed in DNA replication buffer (20 mM HEPES, pH 7.6, 110 mM KCl, 5 mM NaCl, 7 mM $MgCl_2$, 1 mM EGTA, 0.5 mM spermidine, 2 mM DTT, and 0.25% BSA) [27] and ~ 1.5×10^6 nuclei were incubated with 17,000 particles of wild-type AAV per nucleus in 100 μl DNA replication buffer containing 2 mM each of dATP, dGTP, and dTTP, and 20 μCi α^{32}P-dCTP (3000 Ci/mmol, Amersham) for 30 min at 37°C followed by 5 h at 25°C. After centrifugation at 3000 rpm for 3 min, the supernatant was discarded, nuclei resuspended in 100 μl PBS, and low M_r DNA isolated and electrophoresed on native or alkaline 1% agarose gels as described [14]. Following Southern blot transfer of the DNA, the nylon membrane was baked *in vacuo* and autoradiographed. In some experiments, ~ 7×10^6 293 cells were washed and infected with 10,000 particles per cell of wild-type AAV with or without 10 MOI of Ad2 for 2 h at 37°C. Cells were incubated for the indicated time periods before isolation of the nuclei.

ACKNOWLEDGMENTS

This research was supported in part by a Public Health Service grant (HL-58881) from the National Institutes of Health and a grant from the Phi Beta Psi Sorority.

doi:10.1006/mthe.2001.0457, available online at http://www.idealibrary.com on IDEAL

REFERENCES

1. Berns, K. I., and Giraud, C. (1996). Biology of adeno-associated virus. *Curr. Top. Microbiol. Immunol.* **218:** 1–23.
2. Srivastava, A., Lusby, E. W., and Berns, K. I. (1983). Nucleotide sequence and organization of the adeno-associated virus 2 genome. *J. Virol.* **45:** 555–564.
3. Kotin, R. M., *et al.* (1990). Site-specific integration by adeno-associated virus. *Proc. Natl. Acad. Sci. USA* **87:** 2211–2215.
4. Flotte, T. R., and Carter, B. J. (1995). Adeno-associated virus vectors for gene therapy. *Gene Ther.* **2:** 357–362.
5. Kay, M. A., *et al.* (2000). Evidence for gene transfer and expression of factor IX in haemophilia B patients treated with an AAV vector. *Nat. Genet.* **24:** 257–261.
6. Ponnazhagan, S., *et al.* (1996). Differential expression in human cells from the p6 promoter of human parvovirus B19 following plasmid transfection and recombinant adeno-associated virus 2 (AAV) infection: human megakaryocytic leukaemia cells are non-permissive for AAV infection. *J. Gen. Virol.* **77:** 1111–1122.
7. Qing, K., *et al.* (1999). Human fibroblast growth factor receptor 1 is a co-receptor for infection by adeno-associated virus 2. *Nat. Med.* **5:** 71–77.
8. Summerford, C., and Samulski, R. J. (1998). Membrane-associated heparan sulfate proteoglycan is a receptor for adeno-associated virus type 2 virions. *J. Virol.* **75:** 8968–8976.
9. Summerford, C., Bartlett, J. S., and Samulski, R. J. (1999). αVβ5 integrin: a co-receptor for adeno-associated virus type 2 infection. *Nat. Med.* **5:** 78–82.
10. Duan, D., Yue, Y., Yan, Z., Yang, J., and Engelhardt, J. F. (2000). Endosomal processing limits gene transfer to polarized airway epithelia by adeno-associated virus. *J. Clin. Invest.***105:** 1573–1587.
11. Qing, K., *et al.* (1997). Role of tyrosine phosphorylation of a cellular protein in adeno-associated virus 2-mediated transgene expression. *Proc. Natl. Acad. Sci. USA* **94:** 10879–10884.
12. Mah, C., *et al.* (1998). Adeno-associated virus type 2-mediated gene transfer: role of epidermal growth factor receptor protein tyrosine kinase in transgene expression. *J. Virol.* **72:** 9835–9843.
13. Qing, K., *et al.* (2001). Adeno-associated virus type 2-mediated gene transfer: role of cellular FKBP52 protein in transgene expression. *J. Virol.* **75:** 8968–8976.
14. Hansen, J., Qing, K., Kwon, H. J., Mah, C., and Srivastava, A. (2000). Impaired intracellular trafficking of adeno-associated virus type 2 vectors limits efficient transduction of murine fibroblasts. *J. Virol.* **74:** 992–996.
15. Hansen, J., Qing, K. Y., and Srivastava, A. (2001). Adeno-associated virus 2-mediated gene transfer: altered endocytic processing enhances the transduction efficiency in murine fibroblasts. *J. Virol.* **75:** 4080–4090.
16. Sanlioglu, S., *et al.* (2000). Endocytosis and nuclear trafficking of adeno-associated virus type 2 are controlled by rac1 and phosphatidylinositol-3 kinase activation. *J. Virol.* **74:** 9184–9196.
17. Bartlett, J. S., Wilcher, R., and Samulski, R. J. (2000). Infectious entry pathway of adeno-associated virus and adeno-associated virus vectors. *J. Virol.* **74:** 2777–2785.
18. Bartlett, J. S., Samulski, R. J., and McCown, T. J. (1998). Selective and rapid uptake of adeno-associated virus type 2 in brain. *Hum. Gene Ther.* **9:** 1181–1186.
19. Davis, L. I., and Blobel, G. (1986). Identification and characterization of a nuclear pore complex protein. *Cell* **45:** 699–709.
20. Finlay, D. R., Newmeyer, D. D., Price, T. M., and Forbes, D. J. (1987). Inhibition of in vitro nuclear transport by a lectin that binds to nuclear pores. *J. Cell Biol.* **104:** 189–200.
21. Greber, U. F., and Gerace, L. (1995). Depletion of calcium from the lumen of endoplasmic reticulum reversibly inhibits passive diffusion and signal-mediated transport into the nucleus. *J. Cell Biol.* **128:** 5–14.
22. Berns, K. I., and Hauswirth, W. W. (1979). Adeno-associated viruses. *Adv. Virus Res.* **25:** 407–449.
23. Kasamatsu, H., and Nakanishi, A. (1998). How do animal DNA viruses get to the nucleus? *Annu. Rev. Microbiol.* **52:** 627–686.
24. Newmeyer, D. D., and Forbes, D. J. (1990). An N-ethylmaleimide-sensitive cytosolic factor necessary for nuclear protein import: requirement in signal-mediated binding to the nuclear pore. *J. Cell Biol.* **110:** 547–557.
25. Marzluff, W. F. (1990). Preparation of active nuclei. *Methods Enzymol.* **181:** 30–36.
26. Peters, R. (1983). Nuclear envelope permeability measured by fluorescence microphotolysis of single liver cell nuclei. *J. Biol. Chem.* **258:** 11427–11429.
27. Hola, M., Castleden, S., Howard, M., and Brooks, R. F. (1994). Initiation of DNA synthesis by nuclei from scrape-ruptured quiescent mammalian cells in high-speed supernatants of Xenopus egg extracts. *J. Cell Sci.* **107:** 3045–3053.